Evanescent-Mode Coupling of Dual-Mode Rectangular Waveguide Filters

Hsin-Chin Chang and Kawthar A. Zaki, *Fellow, IEEE*

Abstract—**A novel coupling method for dual-mode rectangular waveguide filters is presented and analyzed. Unequal coupling between dual-mode pairs of rectangular cavities is achieved without the need of an iris. This method replaces the iris completely while offering a practical, flexible, and wide range of couplings. Mode matching method is used in the analysis and its accuracy is verified by experiments. A four-pole dual-mode elliptic function filter using this new coupling method is built and tested. Results show excellent agreement with the analysis.**

I. Introduction

CONVENTIONAL dual-mode waveguide filters require cross slot irises to provide coupling between modes in adjacent resonators [1]–[3]. The major drawback of this coupling method is that the dimensions of the slot are determined by a small-aperture approximation [7] that does not provide the required accuracy for this type of application. This means repeated experimental tuning (machining) is needed, which makes irises expensive and creates an engineering bottleneck. Efforts have been made to design a waveguide filter without irises or with a reduced number of irises [4]–[6]. One promising method [6] is to replace the iris with a short waveguide of smaller cross section. The advantage of this method is that an accurate calculation of the coupling coefficient can be made, and the resulting dimensions are reasonable.

The previous work [6] was done in a cylindrical waveguide filter. The coupling waveguide is circular in cross section and hence gives equal coupling for the dual modes. Except for the canonical form [4], unequal coupling is generally required between adjacent cavities. Therefore, additional coupling screws must be added and a tuning procedure must be performed. Furthermore, the amount of coupling increase achievable by the additional tuning screw is limited. Thus a large ratio of coupling between the two orthogonal dual modes cannot be realized.

This paper introduces a configuration which overcomes the above problems. Consider the four-pole dual-mode elliptic function filter shown in Fig. 1, where the arrows denote electric field polarization of the four resonant modes, and the M_{ij}'s are the couplings between them. Note that $M_{14} \neq M_{23}$. To realize couplings M_{14} and M_{23} the coupling structure should be asymmetric to 90° rotation. One possible configuration is to use two rectangular cavities connected by a smaller rectangular waveguide. This is shown in Fig. 2. The addition of coupling screws for M_{12} and M_{34}, frequency fine-tuning screws, and input/output connections provides the complete waveguide filter. Since the mode matching analysis provides precise results of the resonant frequencies of the two dual orthogonal modes, as well as the coupling between the modes, it is possible to design single- or dual-mode filters in this configuration which require no tuning screws. This is particularly attractive at higher microwave and millimeter-wave frequencies, where the additional losses and tuning sensitivity may not be tolerated. This structure is analyzed by the mode matching method. The results is verified by measurements. An experimental four-pole dual-mode elliptic function filter is designed, built, and tested. Measured results show excellent agreement with analysis.

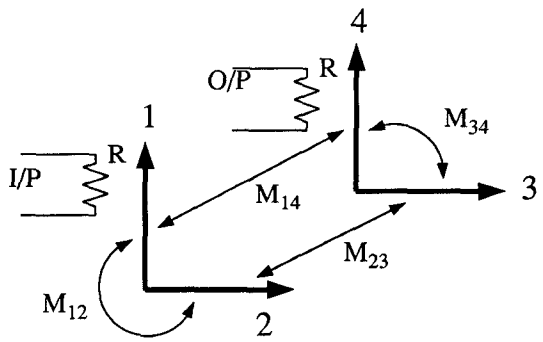

Fig. 1. A symbolic description of a four-pole elliptic function filter.

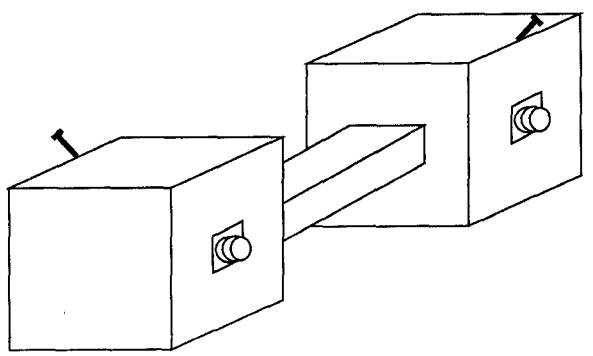

Fig. 2. One possible configuration for realizing the filter in Fig. 1.

Manuscript received October 4, 1990; revised March 26, 1991.

The authors are with the Electrical Engineering Department, University of Maryland, College Park, MD 20742.

IEEE Log Number 9101372.

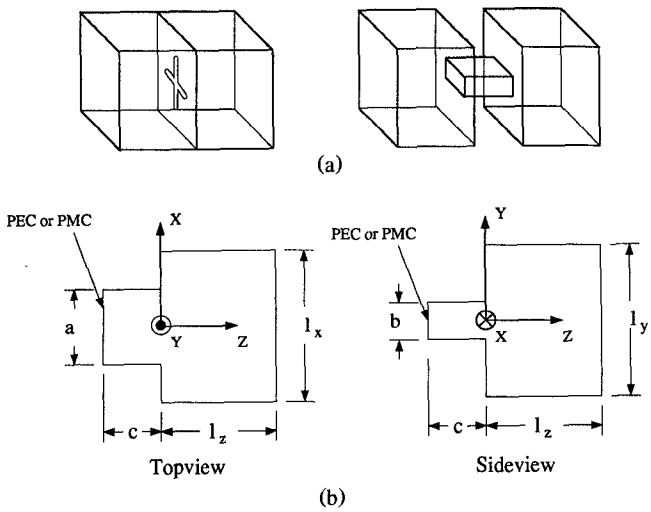

Fig. 3. (a) The conventional (*left*) and the new (*right*) coupling method. (b) the configuration under analysis.

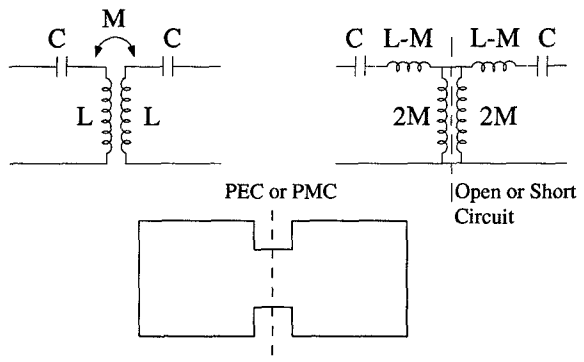

Fig. 4. Two equivalent circuits of the coupling structure.

II. Analysis

The new coupling method introduces a short coupling waveguide of smaller cross section that replaces the cross iris. The comparison is shown in Fig. 3(a). The small coupling waveguide between the two dual-mode rectangular cavities is beyond cutoff over the desired band of the filter such that only evanescent modes can exist. There are three parameters (i.e., the height, width, and length of the coupling waveguide) that can be varied to achieve the two prescribed couplings (i.e., M_{14} and M_{23}). Therefore, the choice of dimensions is very flexible. These dimensions can be adjusted to meet geometric specifications. For the purpose of the analysis, the dual orthogonal mode pairs in each of the two cavities are assumed to be uncoupled (i.e., no 45° coupling screws are present). With this assumption, only the modes of similar polarization in each cavity are coupled, and thus can be analyzed separately. Two equivalent circuits of the coupling structure for one mode in each cavity are shown in Fig. 4, where M is the mutual inductance. There are two resonant frequencies for these circuits, namely f_e and f_m. They can be derived from the symmetry of the structure by placing a perfect electric conductor (PEC) or a perfect magnetic conductor (PMC) on the symmetry plane respectively. The coupling coefficient is shown to be given by

$$k = \frac{M}{L} = \frac{f_e^2 - f_m^2}{f_e^2 + f_m^2}. \tag{1}$$

By placing a PEC or a PMC in the midway plane of the coupling waveguide, only half the structure, shown in Fig. 3(b), together with the coordinates and definition of geometric parameters, needs to be analyzed. The plane $z = -c$ can be either a PEC or a PMC. The mode matching method can be used to analyze the structure in Fig. 3(b), i.e., to calculate f_e (with PEC at the center) and f_m (with PMC at the center). Then (1) is used to obtain the coupling coefficient, k. The half-sections in Fig. 3(b) are divided into two regions:

Region I: $z \geqslant 0$, the cavity.
Region II: $z \leqslant 0$, the coupling waveguide.

Within each region, both TE modes and TM modes (transverse to the z direction) are used to match the boundary at $z = 0$. The H_z fields for the TE modes are, for region I,

$$H_{mn}^{\mathrm{I}z} = \hat{\mu} \cos\frac{m\pi}{l_x}\left(x + \frac{l_x}{2}\right)\cos\frac{n\pi}{l_y}\left(y + \frac{l_y}{2}\right) \cdot \frac{\sinh\gamma_{mn}^{\mathrm{I}}(l_z - z)}{\sinh\gamma_{mn}^{\mathrm{I}} l_z} \tag{2}$$

and for region II,

$$H_{ij}^{\mathrm{II}z} = \hat{\mu} \cos\frac{i\pi}{a}\left(x + \frac{a}{2}\right)\cos\frac{j\pi}{b}\left(y + \frac{b}{2}\right) \cdot \begin{cases} \dfrac{\sin\gamma_{ij}^{\mathrm{II}}(z+c)}{\sinh\gamma_{ij}^{\mathrm{II}} c}, & \text{PEC} \\ \dfrac{\cosh\gamma_{ij}^{\mathrm{II}}(z+c)}{\cosh\gamma_{ij}^{\mathrm{II}} c}, & \text{PMC.} \end{cases} \tag{3}$$

The E_z fields for the TM modes are, for region I,

$$E_{mn}^{\mathrm{I}z} = \sin\frac{m\pi}{l_x}\left(x + \frac{l_x}{2}\right)\sin\frac{n\pi}{l_y}\left(y + \frac{l_y}{2}\right)\frac{\cosh\gamma_{mn}^{\mathrm{I}}(l_z - z)}{\cosh\gamma_{mn}^{\mathrm{I}} l_z} \tag{4}$$

and for region II,

$$E_{ij}^{\mathrm{II}z} = \sin\frac{i\pi}{a}\left(x + \frac{a}{2}\right)\sin\frac{j\pi}{b}\left(y + \frac{b}{2}\right) \cdot \begin{cases} \dfrac{\cosh\gamma_{ij}^{\mathrm{II}}(z+c)}{\cosh\gamma_{ij}^{\mathrm{II}} c}, & \text{PEC} \\ \dfrac{\sinh\gamma_{ij}^{\mathrm{II}}(z+c)}{\sinh\gamma_{ij}^{\mathrm{II}} c}, & \text{PMC.} \end{cases} \tag{5}$$

Notice that for TE modes, m or n can be zero, while for TM modes both m and n must be positive. The transverse fields can be derived from the axial field components through Maxwell's equations. In all the equations

above $\hat{\mu} = j\omega\mu$ and $\hat{\epsilon} = j\omega\epsilon$, μ and ϵ being the permeability and permittivity of the medium within the structure.

On the plane $z = 0$, the boundary condition requires both the transverse electric fields (E_x and E_y) and the transverse magnetic fields (H_x and H_y) to be continuous, i.e.,

$$\sum_{m,n,p} A_{mn}^{p} \vec{E}_{mn}^{\mathrm{I}p} = \sum_{i,j,q} B_{ij}^{q} \vec{E}_{ij}^{\mathrm{II}q} \tag{6}$$

$$\sum_{m,n,p} A_{mn}^{p} \vec{H}_{mn}^{\mathrm{I}p} = \sum_{i,j,q} B_{ij}^{q} \vec{H}_{ij}^{\mathrm{II}q} \tag{7}$$

where the superscripts p and q stand for the TE mode or the TM mode. The A's and B's are the mode coefficients in regions I and II respectively. The $\vec{E}$'s and $\vec{H}$'s are the vector transverse fields at $z = 0$.

Define the cross product of two modes as

$$\langle \vec{E}^{u} \times \vec{H}^{v} \rangle \equiv \int_{\text{cross section}} \left(E_x^{u} H_y^{v} - E_y^{u} H_x^{v} \right) dA. \tag{8}$$

From the orthogonality of eigenmodes, it is known that if both the $\vec{E}$ and $\vec{H}$ fields in (8) are in the same region, all the products vanish unless u and v are the same mode. Taking the cross product of the H field of some mode in region I on both sides of (6) and the cross product of the E field of some mode in region II on both sides of (7) and using the orthogonality relation (8), the following equations are obtained:

$$A_{mn}^{p} \langle \vec{E}_{mn}^{\mathrm{I}p} \times \vec{H}_{mn}^{\mathrm{I}p} \rangle = \sum_{i,j,q} B_{ij}^{q} \langle \vec{E}_{ij}^{\mathrm{II}q} \times \vec{H}_{mn}^{\mathrm{I}p} \rangle \tag{9}$$

$$\sum_{m,n,p} A_{mn}^{p} \langle \vec{E}_{ij}^{\mathrm{II}q} \times \vec{H}_{mn}^{\mathrm{I}p} \rangle = B_{ij}^{q} \langle \vec{E}_{ij}^{\mathrm{II}q} \times \vec{H}_{ij}^{\mathrm{II}q} \rangle. \tag{10}$$

Substituting the A_{mn}^{p} from (9) into (10) gives

$$\begin{aligned} B_{i'j'}^{q'} \langle \vec{E}_{i'j'}^{\mathrm{II}q'} \times \vec{H}_{i'j'}^{\mathrm{II}q'} \rangle &= \sum_{m,n,p} \frac{\sum_{i,j,q} B_{ij}^{q} \langle \vec{E}_{ij}^{\mathrm{II}q} \times \vec{H}_{mn}^{\mathrm{I}p} \rangle}{\langle \vec{E}_{mn}^{\mathrm{I}p} \times \vec{H}_{mn}^{\mathrm{I}p} \rangle} \langle \vec{E}_{i'j'}^{\mathrm{II}q'} \times \vec{H}_{mn}^{\mathrm{I}p} \rangle \\ &= \sum_{i,j,q} B_{ij}^{q} \sum_{m,n,p} \frac{\langle \vec{E}_{ij}^{\mathrm{II}q} \times \vec{H}_{mn}^{\mathrm{I}p} \rangle \langle \vec{E}_{i'j'}^{\mathrm{II}q'} \times \vec{H}_{mn}^{\mathrm{I}p} \rangle}{\langle \vec{E}_{mn}^{\mathrm{I}p} \times \vec{H}_{mn}^{\mathrm{I}p} \rangle} \end{aligned} \tag{11}$$

or, in matrix form,

$$\left(\sum_{m,n,p} \frac{\langle \vec{E}_{ij}^{\mathrm{II}q} \times \vec{H}_{mn}^{\mathrm{I}p} \rangle \langle \vec{E}_{i'j'}^{\mathrm{II}q'} \times \vec{H}_{mn}^{\mathrm{I}p} \rangle}{\langle \vec{E}_{mn}^{\mathrm{I}p} \times \vec{H}_{mn}^{\mathrm{I}p} \rangle} - \langle \vec{E}_{i'j'}^{\mathrm{II}q'} \times \vec{H}_{i'j'}^{\mathrm{II}q'} \rangle \delta_{ii'} \delta_{jj'} \delta_{qq'} \right) \left(B_{ij}^{q} \right) = 0 \tag{12}$$

where unprimed indices i, j, and q are for the columns and the primed ones are for the rows. The δ's are the Kronecker delta function. The (B_{ij}^{q}) is a column vector composed of all the mode coefficients in region II. The rank of the square matrix is the total number of modes taken (the sum of the number of TE and TM modes) in region II. In order to be able to handle it numerically, the infinite matrix in (12) has to be truncated. For example, if the m and n in (2) take N_{Ix}^{TE} and N_{Iy}^{TE} different values, respectively, and the m and n in (4) take N_{Ix}^{TM} and N_{Iy}^{TM} values, then the summation in (12) would be over $N_{Ix}^{\mathrm{TE}} \times N_{Iy}^{\mathrm{TE}} + N_{Ix}^{\mathrm{TM}} \times N_{Iy}^{\mathrm{TM}}$ terms. And if the i and j in (3) take N_{IIx}^{TE} and N_{IIy}^{TE} different values, respectively, and the i and j in (5) take N_{IIx}^{TM} and N_{IIy}^{TM} values, then the rank of the matrix would be $N_{IIx}^{\mathrm{TE}} \times N_{IIy}^{\mathrm{TE}} + N_{IIx}^{\mathrm{TM}} \times N_{IIy}^{\mathrm{TM}}$.

Equation (12) is a homogeneous linear system of equations. In order to have a nonzero solution for the coefficients, the determinant of the matrix in (12) must be zero. The frequencies that satisfy this condition are the resonant frequencies. Both cases for a PEC and a PMC wall at the symmetry plane are calculated. They are used to obtain the coupling coefficients from (1). We can substitute the frequency back into (12) to solve for the coefficients, and then the field distribution inside the cavity is obtained.

III. Results

A program has been developed for the calculation of the coupling coefficient and field distributions. The total fields existing in the resonator at resonance are a combination of TE and TM modes. Therefore, these fields cannot strictly be designated as pure TE or TM modes and are designated as hybrid (HE) modes. However, for calculating the coupling between the two cavities using the small-aperture approximation, the TE_{01} mode is assumed to be the only mode existing in the cavities. The approximate coupling is computed from [7], [8]

$$k = \frac{\lambda^2}{l_z^3 l_x l_y} \frac{M}{1 - \left(\frac{\lambda_c}{\lambda} \right)^2} 10^{-8.19/\lambda_c \sqrt{1 - (\lambda_c/\lambda)^2}} \tag{13}$$

where λ is the free-space wavelength and λ_c is the cutoff wavelength inside the coupling waveguide. M is the magnetic polarizability of the aperture. Figs. 5 and 6 show the variation of the coupling coefficient between two cavities as a function of half the coupling section length (c). In addition to the measured and computed results using the mode matching method, the figures also show the approximated small-aperture coupling coefficient. Conventional coupling measurement methods carry measurement error, inherent in these methods and hardware limitations. We have essentially eliminated these errors by using the reflection coefficient phase measurement method [10]. In this method the frequencies of the zeros and poles of the one-port network (i.e., the 180° and 0° phases of the reflection coefficient) are accurately measured. The coupling coefficient is determined only from frequency measurements. Since a synthesizer is used as the source, frequency measurement errors are essentially eliminated,

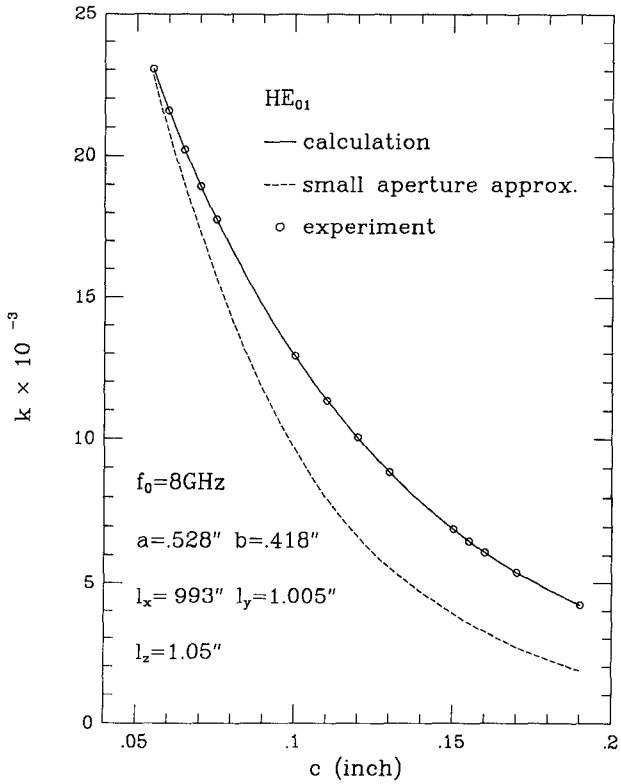

Fig. 5. Comparison of measured coupling coefficient with calculated from different approaches (HE_{01} mode).

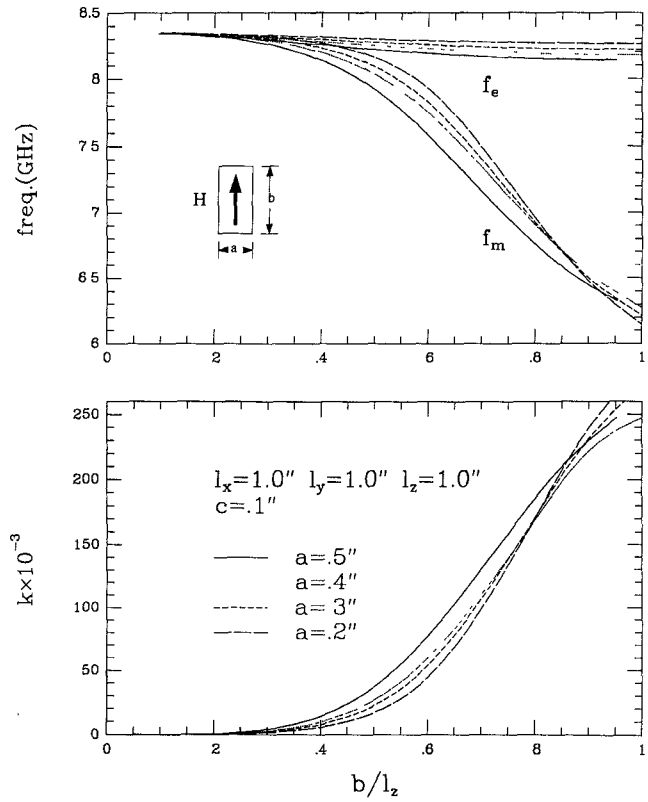

Fig. 7. Variation of resonant frequencies (f_e and f_m mode) and coupling coefficients with coupling waveguide length a.

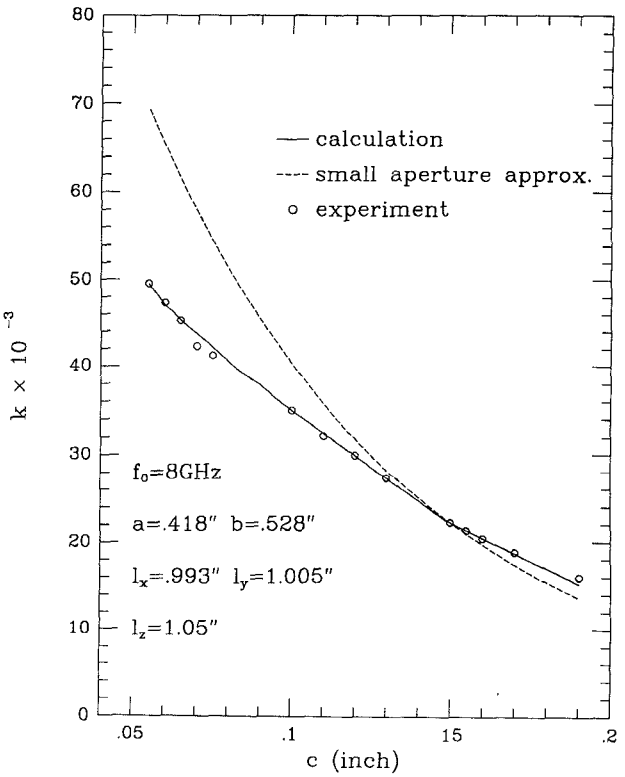

Fig. 6. Comparison of measured coupling coefficient with calculated from different approaches (HE_{01} mode).

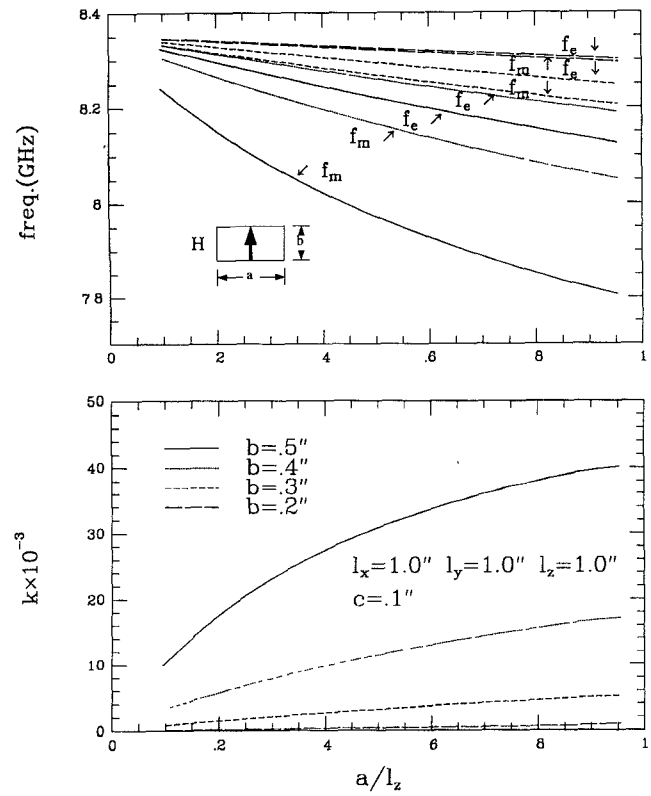

Fig. 8. Variation of resonant frequencies (f_e and f_m mode) and coupling coefficients with coupling waveguide length b.

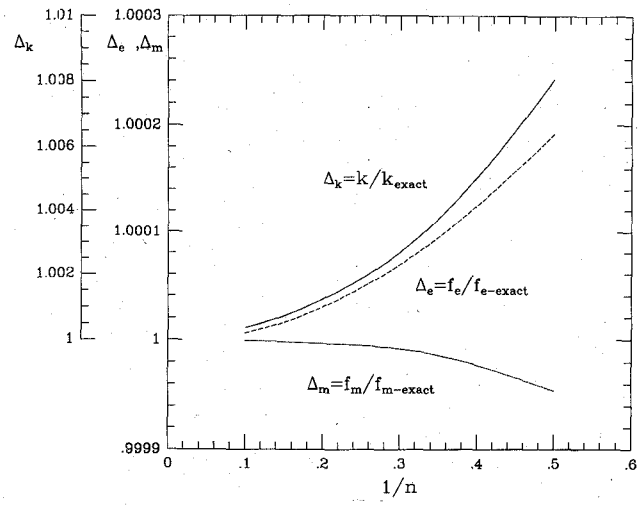

Fig. 9. Convergence behavior of resonant frequencies and coupling coefficient with number of modes used.

thus yielding very accurate coupling measurement. The calculated results using mode matching agree extremely well with the measured results, with an error of less than 1.0%. Figs. 7 and 8 show the variation of the coupling with the height and width (a and b) of the coupling section respectively.

It can be seen that the coupling between the two modes behaves differently with the height and width of the coupling waveguide. In all the figures above, l_z is fixed. These figures show that the proposed coupling method can realize couplings of very wide range and ratio.

The convergences of resonant frequencies and coupling coefficients with the number of modes used in the mode matching are shown in Fig. 9. Assuming $l_x = l_y = l_z = 1$ in., $a = b = 0.5$ in., and $c = 0.1$ in., the numbers of modes in regions 1 and 2 are chosen to be $N_{Ix}^{TE} = N_{Iy}^{TE} = N_{Ix}^{TM} = N_{Iy}^{TM} = 2n$ and $N_{IIx}^{TE} = N_{IIy}^{TE} = N_{IIx}^{TM} = N_{IIy}^{TM} = n$, respectively. Fig. 9 shows that at least $n = 4$ is needed to be within 0.1%. In general, the number of modes used in the two regions should be proportional to their sizes [9]. For example, if $l_x/a = 2$ and $l_y/b = 1$, then $(N_{Ix}^{TE} + N_{Ix}^{TM})/(N_{IIx}^{TE} + N_{IIx}^{TM}) = 2$ and $(N_{Iy}^{TE} + N_{Iy}^{TM})/(N_{IIy}^{TE} + N_{IIy}^{TM}) = 1$.

The H_z and E_z fields on the boundary as obtained from both regions I and II are shown in Fig. 10 and Fig. 11 respectively. These fields indicate how well the boundary conditions are satisfied.

Finally, a dual-mode four-pole elliptic function filter has been designed, built, and tuned. The normalized coupling matrix and I/O impedance are given in (14). The filter is designed to have a center frequency of 7.83 GHz and a bandwidth of 160 MHz. The dimensions of the cavities and coupling section were determined from the mode matching analysis to be $l_x = 0.993$ in., $l_y = 1.005$ in., $l_z = 1.05$ in., $a = 0.528$ in., $b = 0.418$ in., and $c = 0.15$ in. The input and output ports were realized by coaxial probes. The measured responses of the experimental fil-

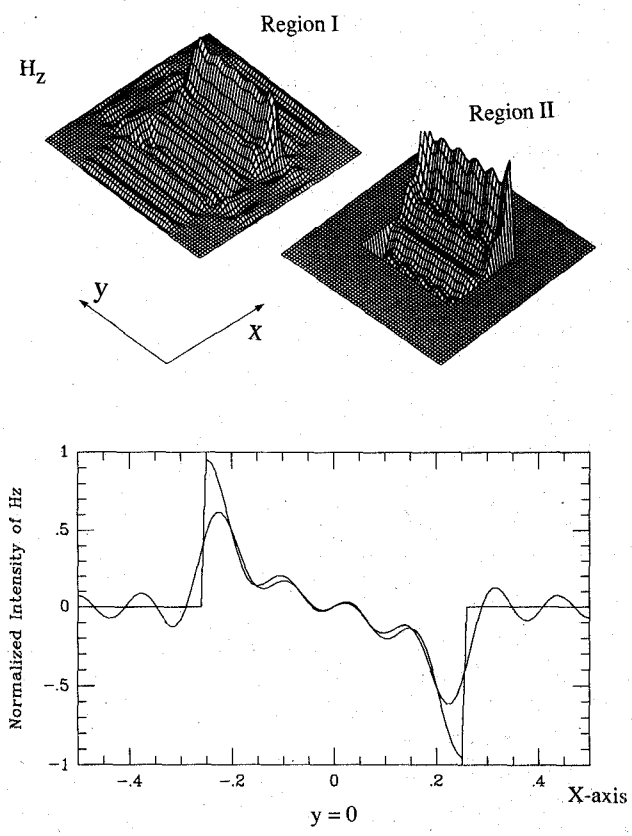

Fig. 10. Matching of H_z field at the boundary $z = 0$.

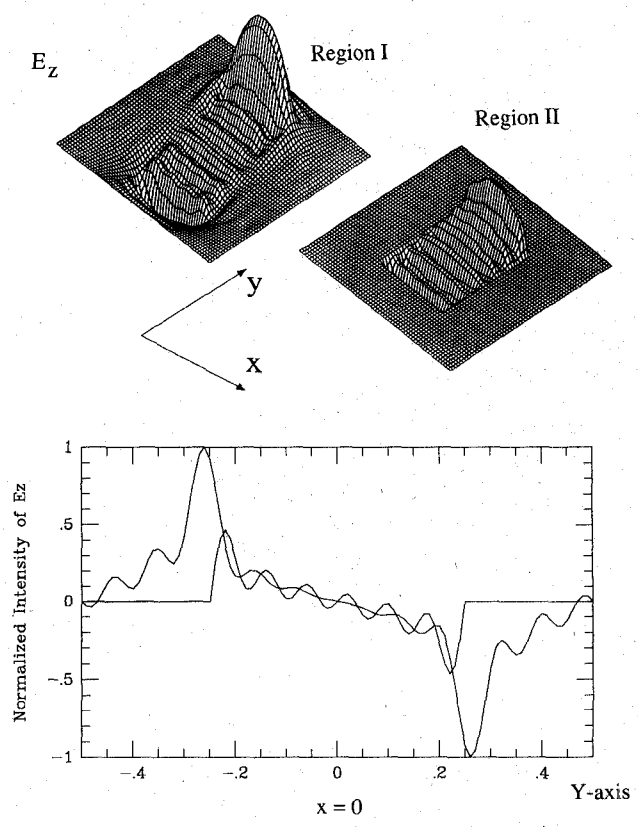

Fig. 11. Matching of E_z field at the boundary $z = 0$.

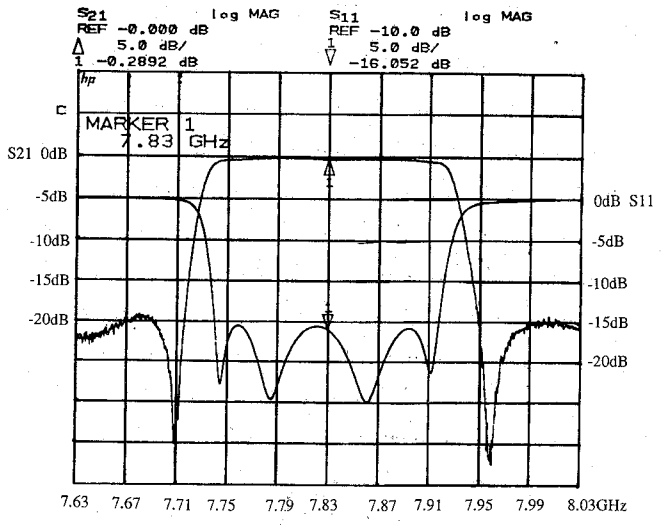

Fig. 12. Measured response for the experimental filter: S_{11} and S_{21}.

ter is shown in Fig. 12:

$$\begin{pmatrix} 0 & 0.81418 & 0 & -0.30145 \\ 0.81418 & 0 & 0.81108 & 0 \\ 0 & 0.81108 & 0 & 0.81418 \\ -0.30145 & 0 & 0.81418 & 0 \end{pmatrix} R=1.0048. \tag{14}$$

IV. Conclusions

A novel coupling method for dual-mode rectangular waveguide filters has been introduced. Mode matching method has been used to analyze the structure and has proved to be extremely accurate, as verified by experiments. Extensive results have been presented to explore the nature of this new coupling method. An experimental dual-mode four-pole elliptic function filter using this new coupling method has been built and its measured performance shows excellent results. This new coupling method has a wide range of practical and potential applications, particularly for high microwave and millimeter-wave frequencies, where tuning screws can be completely eliminated.

References

[1] A. E. Atia and A. E. Williams, "New types of bandpass filters for satellite transponders," *COMSAT Tech. Rev.*, vol. 1, no. 1, pp. 21–43, Fall 1971.

[2] A. E. Atia and A. E. Williams, "Narrow bandpass waveguide filters," *IEEE Trans. Microwave Theory Tech.*, vol. MTT-20, pp. 258–265, Apr. 1972.

[3] S. J. Fiedziusko, "Dual-mode dielectric resonator loaded cavity filters," *IEEE Trans. Microwave Theory Tech.*, vol. MTT-30, pp. 1311–1316, Sept. 1982.

[4] K. A. Zaki, C. Chen, and A. E. Atia, "Canonical and longitudinal dual mode dielectric resonator filters without iris," *IEEE Trans. Microwave Theory Tech.*, vol. MTT-35, pp. 1130–1135, Dec. 1987.

[5] S. W. Chen, K. A. Zaki, and A. E. Atia, "A single iris 8-pole dual mode dielectric resonator filter," in *Proc. 19th European Microwave Conf.*, Sept. 1989, pp. 513–518.

[6] S. W. Chen and K. A. Zaki, "A novel coupling method for dual mode dielectric resonators or waveguide filters," *IEEE Trans. Microwave Theory Tech.*, vol. 38, pp. 1885–1893, Dec. 1990.

[7] H. A. Bethe, "Theory of diffraction by small holes," *Phys. Rev.*, vol. 66, pp. 163–182, 1944.

[8] G. L. Matthaei, L. Young, and E. M. T. Jones, *Microwave Filters, Impedance-Matching Networks, and Coupling Structures*. New York: McGraw-Hill, 1964, ch. 8, pp. 229–243.

[9] P. H. Masterman and P. J. B. Clarricoats, "Computer field-matching of waveguide transverse discontinuities," *Proc. Inst. Elec. Eng.*, vol. 118, no. 1, pp. 51–63, Jan. 1971.

[10] A. E. Atia and A. E. Williams, "Measurements of intercavity couplings," *IEEE Trans. Microwave Theory Tech.*, vol. MTT-23, pp. 519–522, June 1975.

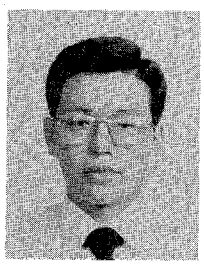

Hsin-Chin Chang was born in Taiwan, R.O.C., on June 13, 1963. He received the B.S. degree in electrical engineering from National Taiwan University in 1985 and the M.S. degree in electrical engineering from the University of Maryland, College Park, in 1989. Since 1987, he has been working as a research assistant in the Microwave Lab, Department of Electrical Engineering, University of Maryland. Currently, he is working toward the Ph.D. degree. His research interests include dielectric-loaded resonator filters, block filter designs, accurate waveguide filter characterization, MIC and MMIC designs, and numerical methods in electromagnetism.

Kawthar A. Zaki (SM'85–F'91) received the B.S. degree (with honors) from Ain Shams University, Cairo, Egypt, in 1962 and the M.S. and Ph.D. degrees from the University of California, Berkeley, in 1966 and 1969, respectively, all in electrical engineering.

From 1962 to 1964, she was a Lecturer in the Department of Electrical Engineering, Ain Shams University. From 1965 to 1969, she held the position of Research Assistant in the Electronic Research Laboratory, University of California, Berkeley. She joined the Electrical Engineering Department, University of Maryland, College Park, in 1970, where she is presently Professor of Electrical Engineering. Her research interests encompass electromagnetics, microwave circuits, optimization, computer-aided design, and optically controlled microwave and millimeter-wave devices.

Dr. Zaki is a member of Tau Beta Pi.